JOURNAL OF GEOPHYSICAL RESEARCH, VOL. 99, NO. D8, PAGES 16,779–16,792, AUGUST 20, 1994

Two-dimensional coupled dynamical/chemical/microphysical simulation of global distribution of El Chichón volcanic aerosols

XueXi Tie
National Center for Atmospheric Research, Boulder, Colorado

Xing Lin[1]
Aeronomy Laboratory, Environmental Research Laboratory, NOAA, Boulder, Colorado

Guy Brasseur
National Center for Atmospheric Research, Boulder, Colorado

Abstract. We have developed a coupled two-dimensional dynamical/chemical/microphysical model to study the global distribution of stratospheric sulfate aerosols. In particular, we use this model to simulate the global distribution of volcanic aerosols after the eruption of El Chichón in Mexico in April 1982. The simulated background aerosol distributions are highly dispersed, while a slight latitudinal gradient is also noticed. The calculated background aerosol surface area and mass are about 0.7 to 1.0 $\mu m^2/cm^3$ and 0.3 to 0.5 parts per billion by mass, respectively, at midlatitude in the northern hemisphere, in fair agreement with available observations. After the eruption of El Chichón in April 1982, the stratospheric aerosol load rapidly increases in the tropics at an altitude of 20 to 25 km. The aerosol area in the tropics reaches a maximum 50 $\mu m^2/cm^3$ in the lower stratosphere, which is about 70–100 times the background aerosol area. Six months after the eruption, volcanic aerosols spread out globally but are still centered in the tropics. One year after the eruption the enhanced aerosol begins to decrease and tends to become uniformly distributed in the lower stratosphere. Two years after the eruption the global aerosol is about 5 times the background aerosol load in the lower stratosphere. The *e*-folding time of the aerosol load is about 10 months in the tropics during the postvolcanic period. Compared to observations (in terms of spatial, temporal, and size distributions), the model quantitatively simulates the evolution of volcanic aerosol clouds. Thus this model could be a useful tool for studying the impacts of volcanic eruptions on stratospheric ozone and climate. Moreover, we find that for a model simulation in which the gas phase SO_2 is the only material ejected by the eruption, the model substantially underestimates the volcanic aerosol load. Thus we expect that the direct ejection of sulfate aerosol particles may be a very important process.

1. Introduction

After the large volcanic eruption of El Chichón in Mexico in April 1982, the total ozone abundance was found to be below the climatological average in December 1982 and in the first few months of 1983 [*Hofmann and Solomon*, 1989]. It has been widely debated whether this reduction in the ozone amount results from heterogeneous reactions on the enhanced aerosol surface provided by the volcanic emission of sulfur or is due to dynamical processes. *Newell and Selkirk* [1988], for example, concluded that the 1982–1983 ozone reduction could have been due to the volcanic eruption, while *Bojkov* [1987] suggested that ozone reduction was probably due to unusual transport effects.

Hofmann and Solomon [1989] analyzed the measured aerosol data and showed that the enhanced aerosol surface area could have reached a maximum of 50 $\mu m^2/cm^3$, a value similar to that encountered inside polar stratospheric clouds. Hofmann and Solomon concluded that heterogeneous reactions occurring on the enhanced aerosol surfaces may have been responsible for at least a portion of the anomalous ozone reduction observed at midlatitudes in early 1983.

Granier and Brasseur [1992] used a two-dimensional (2-D) coupled dynamical/chemical model to study the effect of the El Chichón eruption on the ozone layer. In their study a parameterized volcanic aerosol surface area was used since observations of aerosols did not provide a global distribution of the surface area density. According to their model the ozone reduction due to the heterogeneous reactions on the enhanced aerosol load is approximately 3% at midlatitudes and 7% at high latitudes in the northern hemisphere. On the basis of the parameterized global aerosol distribution and the assumption that the distribution of surface area density remains unchanged during 1 year following the eruption, they concluded that the accuracy of such calculations de-

[1]Also at Cooperative Institute for Research in Environmental Sciences, University of Colorado, Boulder.

Paper number 94JD01157.
0148-0227/94/94JD-01157$05.00

pends on the assumption made for the volcanic clouds after large-scale dispersion of the volcanic material.

In spite of the difficulties in measuring the global distribution of volcanic aerosols, some efforts have been made to simulate the formation and fate of volcanic aerosols. *Turco et al.* [1983], for example, used a one-dimensional microphysical model to assess the atmospheric effects of the Mount St. Helens eruption. From their simulation they found that the effects of the Mount St. Helens emissions on stratospheric ozone were small. A maximum ozone depletion of ~0.2% was predicted for early 1981. *McKeen et al.* [1984] used a chemical/dynamical two-dimensional model to simulate the evolution of the volcanic SO_2 cloud. Because they did not include sulfate microphysical processes in their model, they concentrated their study on the chemical mechanisms inside the volcanic cloud, where injected SO_2 was converted into H_2SO_4. *Pinto et al.* [1989] used a one-dimensional microphysical and chemical model to examine the chemistry of the stratospheric sulfate cloud. Their results suggested that microphysical processes rapidly produce large particles inside the volcanic cloud. Because larger particles settle out faster than smaller ones, they suggested that volcanic effects may be self-limiting due to the faster sedimentation process. *Capone et al.* [1983] have used a two-dimensional model to study sulfate aerosol after the eruption of El Chichón. Their calculations suggest that the residence time of the sulfate aerosol cloud after the eruption exceeds 2 years. *Visconti et al.* [1988] have also used a two-dimensional model to simulate El Chichón aerosols. In their simulations the aerosol is treated as a passive tracer. Their results suggest that aerosol cannot be considered as a passive tracer so that microphysical processes should be considered.

By including a microphysical model of sulfate aerosols in the National Center for Atmospheric Research (NCAR) two-dimensional dynamical/chemical model of *Brasseur et al.* [1990], this study attempts to simulate the global distribution of aerosol both during nonvolcanic periods and after the eruption of El Chichón. The paper is structured in the following way: First, we describe the microphysical formulation included in the two-dimensional model. Then we compare the simulated background aerosol distributions with observed ones. Finally, we address the methods and results of the simulation of global distributions of volcanic aerosol after the eruption of El Chichón.

2. Model Description

The two-dimensional model used in the present study is based on an updated version of the two-dimensional coupled dynamical/chemical model (DCM) described by *Brasseur et al.* [1990]. It accounts for feedback between changing chemical distributions and dynamical variables such as temperature and wind distributions. The resolution of the model is 5° in latitude from 85°N to 85°S and 1 km in altitude from 0 to 85 km. Approximately 110 reactions affecting the oxygen, hydrogen, nitrogen, chlorine, bromine, fluorine, and the sulfur families are taken into account to simulate gas phase chemical processes. The present model does not account for the radiative effects of stratospheric aerosols. Thus the potential interactions between stratospheric aerosols and atmospheric dynamics are ignored. The simulated dynamical features, i.e., winds and temperature, are shown by *Brasseur et al.* [1990]. The overall transport produced by the model in the lower stratosphere can be validated by simulating the dispersion of $^{14}CO_2$ distribution in the lower stratosphere (NASA 2-D model intercomparison, Satellite Beach, 1992). The overall lifetime calculated for this tracer is in the range, although at the lower end, of the values determined by 10 other two-dimensional models involved in the NASA 2-D model intercomparison. With heterogeneous chemistry taken into account, the model simulates the total ozone distribution fairly well compared to the observation; these results are presented by *Granier and Brasseur* [1992].

The microphysical model developed in this study and coupled into the 2D DCM is in many respects similar to the models of *Turco et al.* [1979] and of *Bekki and Pyle* [1992]. The stratospheric aerosols are formed by gaseous sulfur-bearing compounds in the stratosphere. It is generally accepted that the major sulfur source during nonvolcanic periods is provided by carbonyl sulfide (OCS), which is released at the surface and transported into the stratosphere [*Crutzen*, 1976]. OCS is then photolyzed, and the products subsequently oxidize to form SO_2. The conversion from SO_2 to H_2SO_4 is complex and not perfectly understood. *Turco et al.* [1982] suggested that the oxidation of SO_2 in the stratosphere is initiated by the gas phase reaction

$$SO_2 + OH + M \rightarrow HSO_3 + M$$

The conversion from HSO_3 to sulfate is more complicated and uncertain. The initiating pathways include

$$\text{(R1)} \qquad HSO_3 + O_2 \rightarrow HO_2 + SO_3$$

$$\text{(R2)} \qquad HSO_3 + OH \rightarrow H_2O + SO_3$$

$$SO_3 + H_2O \rightarrow H_2SO_4$$

Other possible pathways have been discussed by *McKeen et al.* [1984]. It should be noted that pathway (R1) produces $HO_x(OH + HO_2)$, so that the net effect for the conversion process of SO_2 to H_2SO_4 has no loss for HO_x. However, through pathway (R2), HO_x is lost during the conversion of SO_2 into H_2SO_4. On the basis of the model studies by *McKeen et al.* [1984], pathway (R1) seems dominant. Table 1 lists the gaseous sulfur reactions used in the model with the corresponding rate constants. It should be emphasized that the sulfur chemistry has been simplified, so that it is appropriate only for stratospheric studies.

The microphysical processes introduced in the 2D DCM include heterogeneous nucleation, condensation, evaporation, coagulation, gravitational sedimentation, and washout. Homogeneous nucleation is ignored. Detailed numerical treatments of these processes can be found in the studies of *Turco et al.* [1979, 1982], *Hamill* [1975], *Hoppel* [1976], *Hamill et al.* [1977], *Yue and Hamill* [1979], *Fuchs* [1964], and *Kasten* [1968].

The microphysical processes included in the model can be summarized as follows. The aerosol particles are assumed to be spherical liquid droplets. The size distribution of the aerosol particles is represented by 25 discrete bins covering a range of particle radii from 0.01 μm to 2.56 μm, with particle volume doubling from one bin to the next. The condensation nuclei (CN) are considered to originate at the Earth's surface with a radius of 0.01 μm. We have assumed that CN are uniformly distributed at the surface, with a

Table 1. Reactions of Sulfur Compounds

Reaction	Rate, $cm^3\ s^{-1}$	Reference
$OCS + h\nu = S + CO$		*JPL* [1990]
$S + O_2 = SO + O$	2.3×10^{-12}	*JPL* [1990]
$OCS + O = SO + CO$	$2.3 \times 10^{-11} \exp(-2200/T)$	*JPL* [1990]
$SO + OH = SO_2 + H$	8.6×10^{-11}	*JPL* [1990]
$SO + ClO = SO_2 + Cl$	2.8×10^{-11}	*JPL* [1990]
$SO + O_2 = SO_2 + O$	$2.6 \times 10^{-13} \exp(-2400/T)$	*JPL* [1990]
$SO_2 + OH + M = HSO_3 + M$	$3.0 \times 10^{-31} (T/300)^{-3.3}[M]$	*JPL* [1990]
$HSO_3 + OH = SO_3 + H_2O$	9.0×10^{-13}	*Turco et al.* [1979]
$HSO_3 + O_2 = SO_3 + HO_2$	$1.3 \times 10^{-10} \exp(-330/T)$	*JPL* [1990]
$SO_3 + H_2O = H_2SO_4$	6.0×10^{-15}	*JPL* [1990]
$H_2SO_4 \rightarrow$ washout		*Turco et al.* [1979]

$[M]$ is the air density (cm^{-3}) and T is the temperature (kelvins). JPL, Jet Propulsion Laboratory.

concentration of 1500 particles/cm^3 [*Turco et al.*, 1979]. The aerosol particles and CN are transported in the same fashion as the other gaseous chemicals. When the CN are transported into the stratosphere and when the ambient H_2SO_4 is saturated, a heterogeneous nucleation takes place, with a nucleation time constant of 10^6 s [*Turco et al.*, 1979]. After nucleation the aerosol particles start to grow by heterogeneous condensation and Brownian coagulation processes.

The heteromolecular condensation of particles has been studied by *Hamill* [1975], *Hoppel* [1976], *Hamill et al.* [1977], and *Yue and Hamill* [1979]. It has been shown that the growth rate of a particle is essentially limited by the rate at which H_{2SO_4} molecules impinge on it. If the partial pressure of gaseous H_2SO_4, $p_{H_2SO_4}$, at a given temperature T is greater than the saturation vapor pressure at the surface of the particle $n^0_{H_2SO_4}$, the particle absorbs H_2SO_4 molecules from its environment; otherwise, the mass of H_2SO_4 included inside the particles remains constant or decreases if H_2SO_4 evaporates from the particle. Absorption or evaporation of H_2O is assumed to be instantaneous, so that a proper weight percentage of H_2SO_4 is maintained inside the particle. Under these conditions the growth rate of the particles in the ith bin can be expressed as [*Hamill*, 1975]

$$\partial r_i/\partial t = \alpha\beta\nu \tag{1}$$

where r_i is the aerosol radius corresponding to bin i; β is the impinging rate at which gaseous H_2SO_4 molecules collide on a surface of unit area; ν is the volume that a single H_2SO_4 molecule would occupy in solution including volume occupied by ambient water molecules; and α is the sticking coefficient of H_2SO_4, assumed here to be unity [*Turco et al.*, 1979].

The impinging frequency β is given by [*Hamill*, 1975; *Yue and Hamill*, 1979]

$$\beta = (n_{H_2SO_4} - n^0_{H_2SO_4})(k_bT/2\pi m_a)^{1/2} \tag{2}$$

with k_b being Boltzmann constant and m_a the mass of a H_2SO_4 molecule. The saturation vapor pressure at the surface of the particle $n^0_{H_2SO_4}$ is calculated according to the method presented by *Ayers et al.* [1980]. Volume ν in (1) is determined from the weight percentage of H_2SO_4 in solution. According to *Steele and Hamill* [1981] and *Hofmann and Oltmans* [1992], the weight percentage W (percent) in the lower stratosphere is a function of the surrounding temperature and humidity and can be expressed by

$$W = 100 - (W_t + aP_w) \tag{3a}$$

where P_w is the partial pressure of surrounding water vapor (in millipascals); W_t (percent) and a can be expressed by

$$W_t = W_{t0} \exp(-T/T_0) \tag{3b}$$

$$a = a_0(T - 180)^{-b} \tag{3c}$$

where T is ambient temperature (kelvins), $W_{t0} = 1866\%$, $T_0 = 50.9$ K, $a_0 = 12.39$, and $b = 1.37$.

The time τ needed for a particle of radius r_i to grow from size r_i to size r_{i+1} ($r_{i+1} > r_i$) can be calculated by integrating (1), so that

$$\tau = (r_{i+1} - r_i)/\beta\nu$$

τ can be regarded as the lifetime of a particle in the ith bin associated with condensational growth. Therefore the condensational rate of the number density of particles in the ith bin, $\partial n/\partial t|_{i,\text{cond}}$, can be calculated as

$$\partial n/\partial t|_{i,\text{cond}} = n_{i\mp1}/\tau_{i\mp1} - n_i/\tau_i \tag{4}$$

with n_i being the number density of the particles in the ith bin.

In the model only diffusive coagulation is taken into account since gravitational coagulation is relatively unimportant [*Turco et al.*, 1979]. The coagulation tendency leading to particles in the ith bin, $\partial n/\partial t|_{i,\text{coag}}$, is provided by the rate at which smaller particles coagulate with each other to form new particles of sizes that fit in the ith bin, $T_{\text{in},i}$, minus the rate at which the ith group particles coagulate with other particles to form new particles of larger sizes. Thus

$$\partial n/\partial t|_{i,\text{coag}} = T_{\text{in},i} - T_{\text{out},i} \tag{5}$$

where $T_{\text{out},i}$ and $T_{\text{in},i}$ can be expressed by

$$T_{\text{out},i} = \sum_{j=1}^{25} K_{ij}n_in_j \tag{6}$$

and

$$T_{\text{in},i} = \sum_{jk} K_{jk}n_kn_j \tag{7}$$

if $k < j < i$ and the radius fitted for the ith bin as the result of coagulation is expressed by $r_i = (n_k/n_j r_k^3 + r_j^3)^{1/3}$. Note that in (7) only those coagulations which produce particles of sizes at the ith bin are counted in the production term due to coagulation. In (6) and (7) the coagulation kernel K is calculated according to *Twomey* [1977]:

$$K_{ij} = 2k_B T/3\eta(2 + r_i/r_j + r_j/r_i) \quad (8)$$

where η is kinematic viscosity.

When aerosols grow to a size of a few microns, gravitational sedimentation becomes important. Some aerosol particles are returned to the troposphere by gravitational settling. The gravitational sedimentation rate for each ith bin is determined by

$$\partial n/\partial t|_{i,\text{sed}} = \partial(\Phi_i)/\partial z \quad (9)$$

where $\Phi_i = n_i w_i$ is the vertical flux of particles, and w_i is terminal velocity of aerosols in the ith bin, which is calculated according to *Kasten* [1968]:

$$w_i = (\tfrac{2}{9})(\rho r_i^2 g/\eta)[1 + (\lambda/r_i)(A + B \exp\{-Cr_i/\lambda\})] \quad (10)$$

In this expression, ρ is the mass density of the aerosol, g is gravitational acceleration, λ is the molecular free length, and A, B, and C are constants, specified by *Kasten* [1968].

As indicated by (10), the calculated terminal velocity is a function of altitude and particle size. For a 1-μm particle at approximately 20 km the terminal velocity is about 10 km/yr, corresponding to a settling time out of the stratosphere of about 1 year. Because the focus of this paper is on stratospheric aerosols, complex tropospheric microphysics is not introduced in the model. Therefore the only aerosol particles present in the troposphere are condensation nuclei (CN). Thus aerosol particles are assumed to be instantaneously washed by rainfall or evaporated into CN. The first-order loss rate for washout process in the troposphere suggested by *Turco et al.* [1979] is

$$R_w = 1.2 \times 10^{-5}(1 - z/z_T) \text{ in unit of } (s^{-1})$$

where z (kilometers) is the altitude and z_T (kilometers) is the tropopause altitude adopted in the 2-D model.

The fact that important microphysical processes are neglected in the troposphere represents a shortcoming of the model. However, as concluded by *Bekki and Pyle* [1992], this simplification is not expected to be critical for the simulation of stratospheric aerosols because the lifetimes of tropospheric sulfuric acid particles and gaseous sulfuric acid are probably so short that they do not represent very substantial sources for the stratospheric aerosol layer. As will be shown in the following discussion, this conclusion might have to be revised, since tropospheric microphysical processes may contribute to the presence of large aerosol particles in the tropical lower stratosphere.

3. Simulation of Background Aerosols

The global distribution of background aerosols present during nonvolcanic periods is governed by atmospheric transport, chemical reactions, and microphysical processes. Background aerosols are produced primarily as a result of carbonyl sulfide (OCS) photolysis [*Crutzen*, 1976] and SO_2 oxidation. The initial OCS concentration adopted in the model is 4.5 ppb at the lower boundary and decreases exponentially with altitude according to the estimation by *Turco et al.* [1982]. The two important sulfate aerosol properties, total surface area and mass, are predicted in the model. The total aerosol surface area density A (square micrometers per cubic centimeter) is defined as

$$A = \int 4\pi r^2 n(r)\, dr$$

which is a key parameter in determining the rate of heterogeneous conversions of N_2O_5 and $ClONO_2$ on the sulfate aerosols. The aerosol mass is a key parameter for the evaluation of the sulfate aerosol budget. Because the comparison between calculated and observed background aerosol could provide useful information for validating the representation of the transport, chemistry, and microphysics in the model, we first compare the calculated background aerosol with the observations.

Figure 1 presents the comparison of calculated aerosol surface area density with data deduced from the satellite observations (stratospheric aerosol and gas experiment II (SAGE II) [*World Meteorological Organization* (*WMO*), 1992]. The calculations show latitudinal and vertical distributions in fair agreement with available observations. Both observations and calculations are characterized by higher surface areas near the poles (about 1.75 μm^2 cm^{-3} at the north pole and about 1.5 μm^2 cm^{-3} at the south pole) and lower surface areas in the tropics (0.5 μm^2 cm^{-3} in the model against 0.75 μm^2 cm^{-3} in the observations). We note

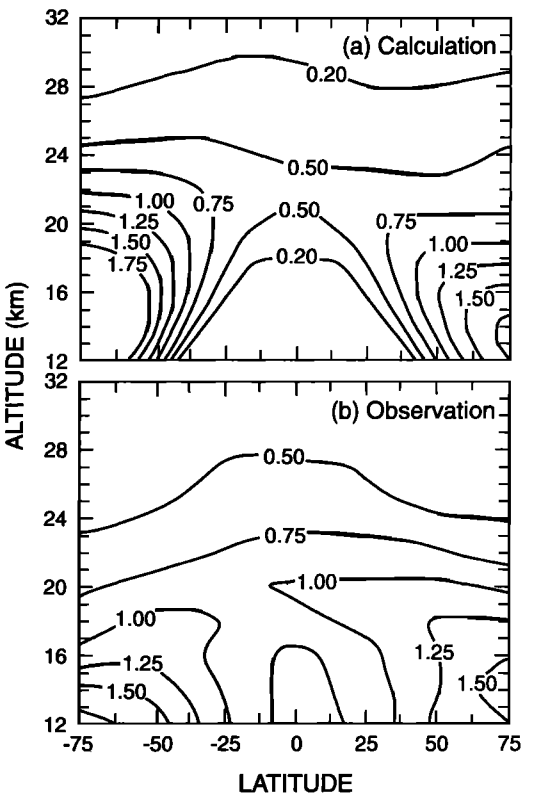

Figure 1. Comparison between simulated and measured March background total aerosol surface area density (square micrometers per cubic centimeter). The observed satellite data are representative of March 1979 [*WMO*, 1992].

that the calculated surface area is about 0.25 μm^2 cm^{-3} less than the observed values in the tropics, perhaps because tropospheric microphysics is neglected in the model. Large sulfate aerosol particles, which are not rapidly evaporated, could be transported from the upper troposphere into the rising branch of the Hadley cell (see Figure 2). Another possible cause for the discrepancy between the model and the observations could be related to the intensity of the Hadley cell as represented in the model. A recent intercomparison of the ^{14}C distributions calculated by 11 two-dimensional models (including the NCAR model) has revealed that upward transport in the tropics is generally too strong in most models (including the NCAR model). This problem could cause a substantial fraction of the aerosols to evaporate near 35–40 km altitude (where the temperature is relatively high) and lead to an underestimation of the aerosol load in the tropics.

We also note that the observations show a slightly larger background aerosol surface area in the northern hemisphere, whereas the calculation shows a slightly larger surface area in the southern hemisphere. This difference could be due to anthropogenic sources of sulfur (such as the aircraft emissions). According to *Bekki and Pyle* [1992], the emission of sulfur by subsonic aircraft could increase the aerosol mass by as much as 60% in the northern hemisphere. These potentially significant, but uncertain, aircraft emissions are ignored in our model.

The meridional distribution of background aerosol area determined in our model is similar to the results obtained by

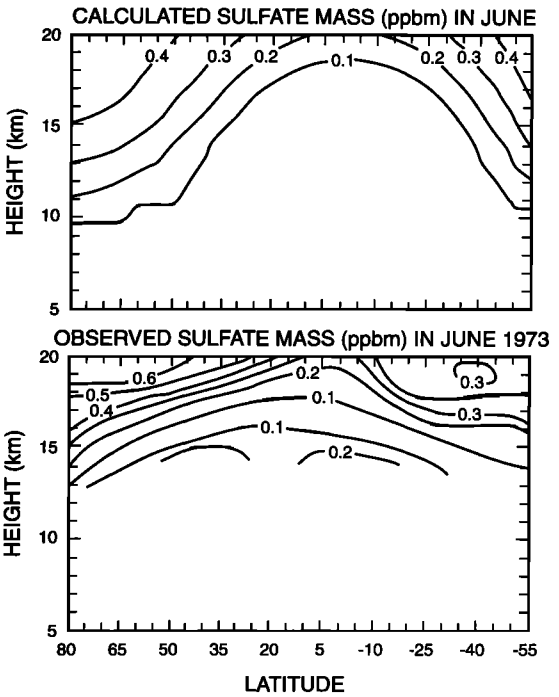

Figure 3. Comparison between calculated and measured aerosol sulfate mass (parts per billion by mass). The data measured in June 1973 [*Sedlacek et al.*, 1983] are representative of background conditions.

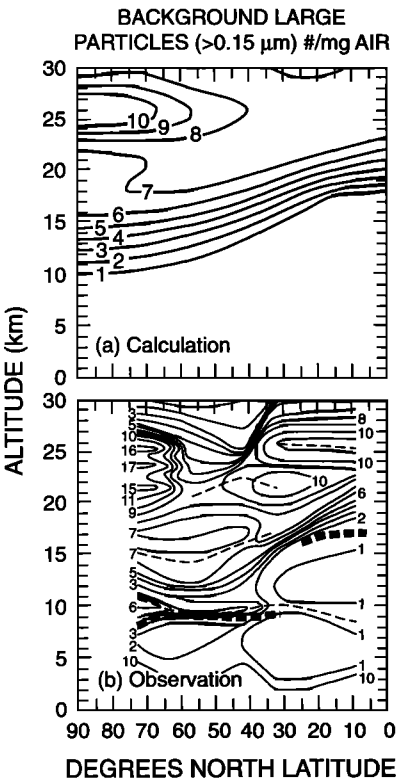

Figure 2. Comparison between calculated and measured density of total large particles (>0.15 μm) (number of particles per milligrams of air). The measurements correspond to March 1973 [*Rosen et al.*, 1975] and are representative of background conditions.

Bekki and Pyle [1992], although the values derived by their model are smaller than those obtained in our model results and than the observations [*WMO*, 1992]. In their model calculation, *Bekki and Pyle* [1992] report an aerosol surface area of 0.3 μm^2 cm^{-3} in the tropics and 0.7 μm^2 cm^{-3} at the poles and suggest that the discrepancy may be due to uncertainties associated with the observation of the small particles by satellites.

Figure 3 presents a comparison of the calculated sulfate mass density (parts per billion by mass, ppbm) with airborne observations [*Sedlacek et al.*, 1983]. The observations took place over a period of 10 years from 1971 to 1981. During this period, several volcanic eruptions took place. After carefully examining the data, *Sedlacek et al.* [1983] concluded that data collected in June 1973 could be representative of "background" conditions. Both observations and calculations show slightly higher aerosol mass densities at high latitudes than in the tropics. The observed mean value is 0.30 ppbm, while the calculated mean is 0.29 ppbm in the region where the observation took place (see Figure 3).

The above comparisons between model results and measurements suggest that for nonvolcanic conditions, the model simulation is satisfactory, although it seems to underestimate the aerosol load in the lower tropical stratosphere.

During large volcanic eruptions, sulfur compounds and particles are often directly injected into the lower stratosphere. We expect therefore that after large eruptions, the microphysical processes in the troposphere are less important than those in the lower stratosphere. We will now use the model to derive the global aerosol distribution following the eruption of El Chichón in 1982.

Table 2. Experiment Design

Experiment	Total Emission of Sulfate, Tg	Total Emission of Gas Phase SO_2, Tg	Total Emission of Sulfate Aerosols, Tg	Emission Altitude, km	Emission Latitude
EXP1	7	4.6 (7 Tg sulfate)	0	19–26	5°S to 15°N
EXP2	7	3.6 (5.5 Tg sulfate)	1.5	19–26	5°S to 15°N
EXP3	11	7.2 (11 Tg sulfate)	0	19–26	5°S to 15°N

4. Simulation of El Chichón Volcanic Aerosols

After the eruption of El Chichón (Mexico) in April 1982, observations of the injected aerosol cloud were made by several groups [*Hofmann and Rosen*, 1984; *Hofmann and Solomon*, 1989; *Mroz et al.*, 1983, 1984; *McCormick and Swissler*, 1983; *Vedder et al.*, 1983]. These observations will be used to validate the model and its capability to simulate stratospheric perturbations caused by large volcanic eruptions.

4.1. Description of Model Simulations

Volcanic eruptions release into the atmosphere large amounts of chemical compounds such as SO_2, H_2S, H_2SO_4, H_2O, ash, HCl, and sulfate aerosols [*Turco et al.*, 1983; *Devine et al.*, 1984; *Cadle et al.*, 1976]. Accurate estimation of the emissions is difficult. Emissions of total sulfur S (SO_2, H_2SO_4, sulfate aerosols) can, however, be deduced approximately from the observed global aerosol mass. Because most of the sulfur released during the eruption is believed to be converted into sulfate particles [*Winker and Osborn*, 1992], the total mass observed after several months is a good representation of the total emission. According to the measurements, the total amount of sulfate ejected by El Chichón is estimated to range from 5 Tg (1 Tg = 10^{12} g) to 12 Tg [*Mroz et al.*, 1983, 1984; *McCormick et al.*, 1984; *McKeen et al.*, 1984]. There is, however, some debate concerning the importance of direct emission of sulfate particles. Several measurements suggest that sulfate particles are present in the vicinity of active volcanic plumes [*Cadle et al.*, 1969; *Hobbs et al.*, 1978; *Woods and Chuan*, 1982; *Rose et al.*, 1982], while other measurements show that gas phase SO_2 emission greatly exceeds the emission of condensed sulfate [*Cadle et al.*, 1979; *Murrow et al.*, 1980]. Recent measurements [*Deshler et al.*, 1992] indicate that sulfate particles are formed by homogeneous nucleation during the initial stage of volcanic eruption.

Because the relative emissions by El Chichón of gas phase SO_2 and aerosol particles are not well quantified, assumptions have to be made in the model. Consistent with the observations which suggest that there is a large increase in the concentration of SO_2 at the initial stage of the volcanic cloud [*Winker and Osborn*, 1992; *Vedder et al.*, 1983; *Goldman et al.*, 1992], we first assume that the largest sulfur emission is in the form of gas phase SO_2. Some studies have also shown that immediate increases of aerosol particles could play an important role in the microphysics of the volcanic plume [*Turco et al.*, 1983; *Deshler et al.*, 1992]. We therefore assume in a second case that the eruption also produces a small amount of sulfate particles. Finally, we assume that a total of 7 Tg of sulfate is ejected by the El Chichón eruption at latitudes ranging from 5°S to 15°N at altitudes of 19 to 26 km. The location of the emission is estimated on the basis of measurements made during the initial stage of the El Chichón eruption [*McCormick and Swissler*, 1983; *Hirono and Shibata*, 1983; *Mroz et al.*, 1984].

On the basis of the above assumptions, we have performed different simulations of the global aerosol distribution and have studied the effects of possible direct ejection of sulfate particles. In experiment 1 (EXP1) we assume that all sulfur (7 Tg) is emitted from El Chichón in the gas phase SO_2 and that SO_2 converts gradually to the sulfate aerosols as a result of chemical and microphysical processes. In experiment 2 (EXP2) we assume that 5.5 Tg of sulfate is released as gas phase SO_2, while 1.5 Tg of sulfate is ejected as condensed sulfate particles with radii ranging from 0.01 μm to 2.5 μm. Table 2 lists the details of the emission scenarios for the two experiments.

4.2. Aerosol Mass Distributions

First, we compare the calculated aerosol sulfate mass distributions to the airborne measurements reported by *Mroz et al.* [1983, 1984]. Note that our model provides two-dimensional, zonally averaged results, while all measurements are taken at specified longitudes. Following the eruption of El Chichón, high-altitude aircraft sampled the aerosol mass at latitudes ranging from 10°S to 90°N and at heights ranging from 12 km to 20 km. The measurement and model results are shown in Figures 4, 5, and 6. Approximately 4 months after the eruption (see Figure 4a) the measured aerosol sulfate mass increases from background value (less than 1 ppbm) to about 20 ppbm at the center of the volcanic cloud (around 10°N latitude and 20 km altitude). In the case of the model simulation (EXP1) (Figure 5a) the aerosol sulfate mass increases to only about 5 ppbm. However, in EXP2 the aerosol sulfate mass increases to about 20 ppbm, a value similar to the observations. In other words, the observation shows a rapid increase of sulfate aerosols shortly after the volcanic eruption. Such rapid effect cannot be simulated if only gas phase SO_2 is injected into the stratosphere during the eruption. In contrast, the rapid increase of sulfate aerosols in the initial stage of the volcanic eruption is well represented in EXP2, in which the ejection of aerosol particles not only directly increases the aerosol mass but also effectively provides surfaces to accelerate the condensation processes. Thus a fast growth of aerosols at the center of the cloud produced by the eruption occurs in EXP2. Six months after the eruption, measurements show that the growth in the aerosol sulfate mass is not yet significant, but northward displacement of the center of cloud is noticeable (Figure 4b). In both experiments (Figures 5b and 6b) the aerosol sulfate mass has slightly grown and is also transported northward. Again, because small amounts of aerosols have been formed at the initial stage of the cloud dispersion, the aerosol mass in EXP1 is smaller than suggested by the measurement. The agreement between model and observation is significantly improved in EXP2. Approx-

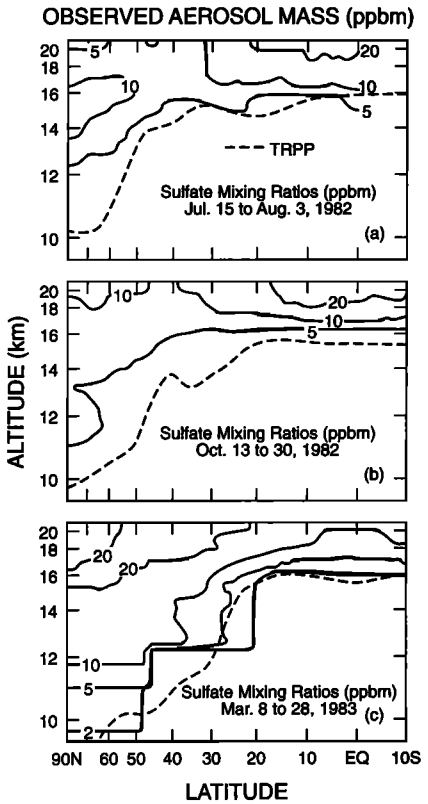

Figure 4. Aerosol sulfate mass density (parts per billion by mass) measured by *Mroz et al.* [1983] in the lower stratosphere after the El Chichón eruption. TRPP, tropopause.

imately 1 year after the eruption, both measurements and model results show that gravitational sedimentation and transport processes have taken place and have played an important role. Large amounts aerosols are found in the

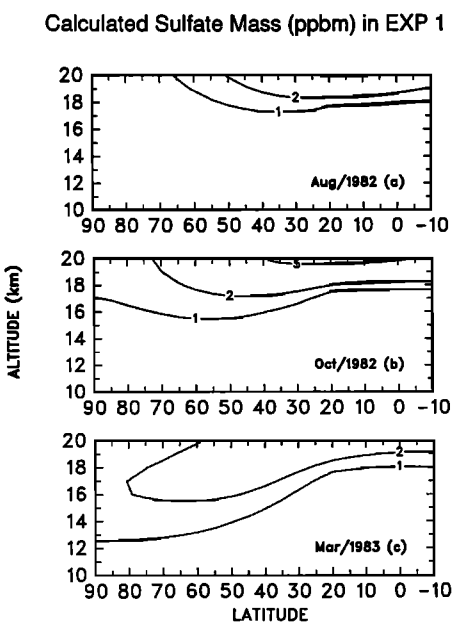

Figure 5. Aerosol sulfate mass density (parts per billion by mass) calculated in the lower stratosphere after the El Chichón eruption (EXP1).

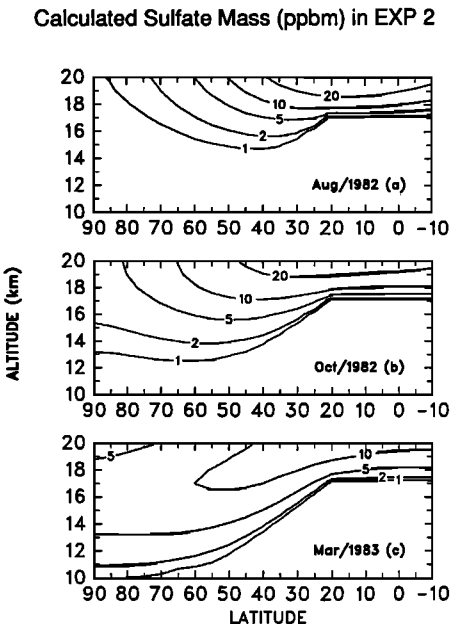

Figure 6. Aerosol sulfate mass density (parts per billion by mass) calculated in the lower stratosphere after the El Chichón eruption (EXP2).

polar regions and at lower altitudes (Figures 4c, 5c, and 6c). Generally, the aerosol sulfate mass simulated in EXP2 is comparable to the observations, while it is less than the observation in EXP1.

4.3. Vertical Distribution of Aerosol Mass and Area

We now compare the vertical distribution of the calculated aerosol sulfate mass and area with the observations. The observational data used for this comparison are provided by balloon measurements reported by *Mroz et al.* [1984] at 30°N and *Hoffman and Solomon* [1989] at 41°N. Because the measurements took place at midlatitudes, transport processes have significantly affected the distribution of the volcanic aerosols. *Mroz et al.* [1984] measured the aerosol sulfate mass at 30°N in New Mexico from August to November 1982, i.e., 4–5 months after the eruption of El Chichón. The measurements and simulation are shown in Figure 7. Comparing calculations to observations, both experiments exhibit a maximum at 23 km, but the simulated maximum in EXP1 (10 ppbm) is significantly smaller than the observed one (50 ppbm), while the maximum obtained in EXP2 (40 ppbm) is closer to the observation.

Hofmann and Solomon [1989] reported total aerosol surface area density measured at 41°N in Wyoming during January 1983, approximately 9 months after the El Chichón eruption. The measurements and simulation results are compared in Figure 8. We first note that the maximum in the aerosol surface area in both measurements and simulations is located at 20 km, which is lower than that for the aerosol mass shown in Figure 7. The decrease with altitude of the aerosol maximum could be due to the fact that 9 months after the eruption (4–5 months in Figure 7), large particles produced by coagulation and condensation have been transported downward by gravitational sedimentation. In the observation and in the EXP1 and EXP2 simulations the aerosol area has increased from 0.7 μm^2 cm^{-3} under back-

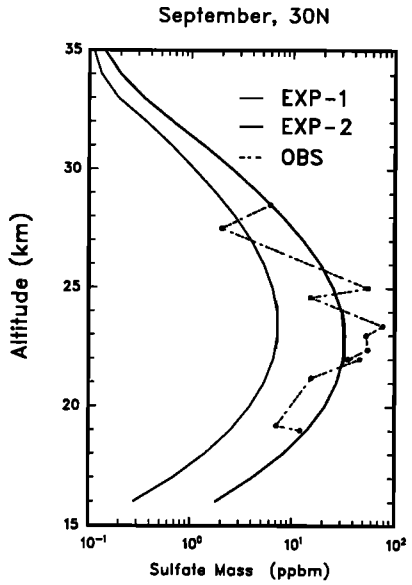

Figure 7. Comparison between measured and calculated aerosol sulfate mass density (parts per billion by mass) at 30°N in the lower stratosphere after El Chichón eruption (September 1982). Measured data are from August to November 1982 by *Mroz et al.* [1984].

ground conditions to about 20 μm^2 cm^{-3}, 6 μm^2 cm^{-3}, and 30 μm^2 cm^{-3} at 20 km, respectively. When comparing simulations with observations, EXP1 underestimates the aerosol surface area, while EXP2 overestimates it.

4.4. Time Evolution of Volcanic Aerosols

Figures 9 and 10 show the temporal evolution in the peak values of mass and surface area density near 40°N. The measurements [*Hofmann and Rosen*, 1984; *Hofmann and Solomon*, 1989] indicate that 10 months after the eruption,

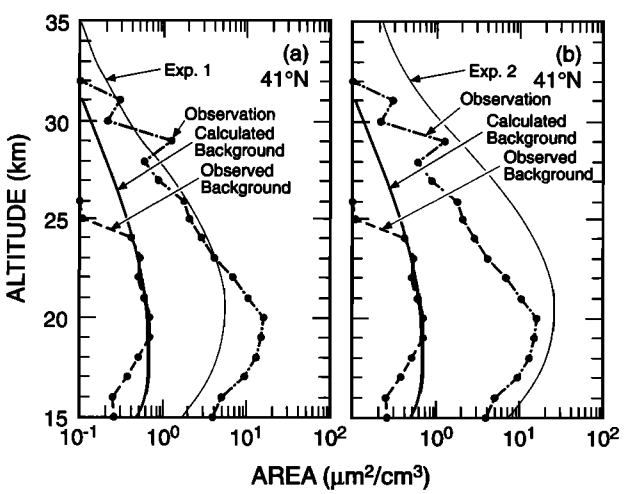

Figure 8. Comparison between measured and calculated aerosol total surface area density (square micrometers per cubic centimeter) in the lower stratosphere near 40°N after El Chichón eruption. Calculations are representative of January 1983. Calculated and measured background conditions are also shown. Measured data are from *Hofmann and Solomon* [1989].

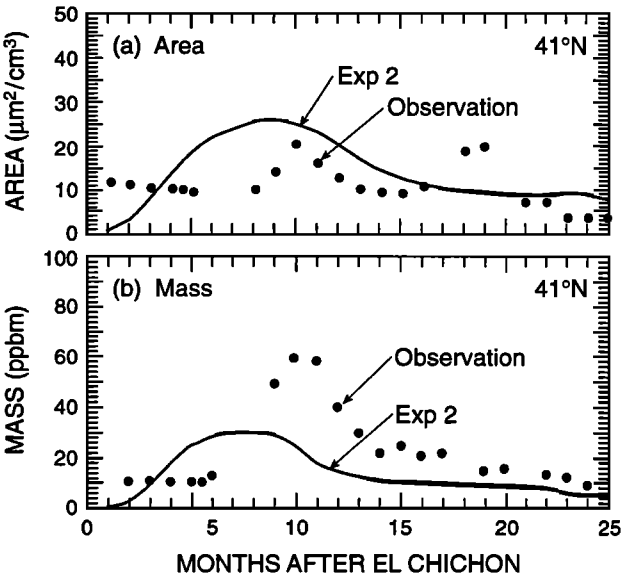

Figure 9. Measured and calculated (EXP2) aerosol peak surface area (square micrometer per cubic centimeter) and peak aerosol mass density (parts per billion by mass) as a function of time after El Chichón eruption near 40°N. Measured aerosol surface area is from *Hofmann and Solomon* [1989], and measured aerosol mass is from *Hofmann and Rosen* [1984].

the aerosol area and mass reach their maximum values. The observed maximum area density is about 20 μm^2 cm^{-3}, and the maximum mass density is about 60 ppbm. These values are approximately 30 to 100 times larger than the background values. Compared to the observations, the calculated area

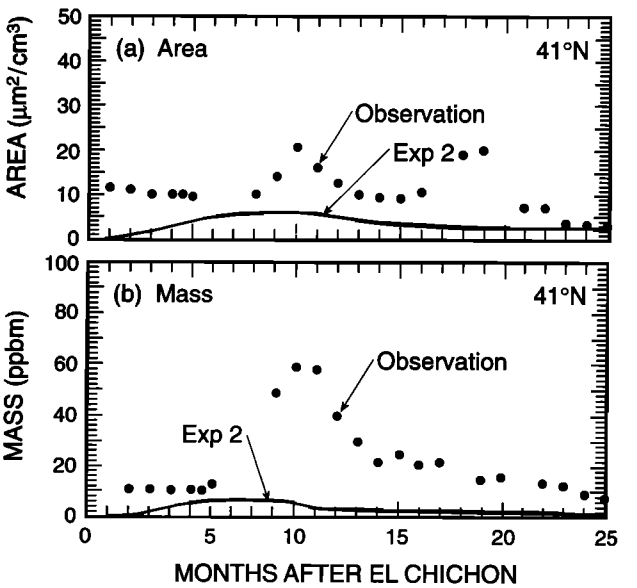

Figure 10. Measured and calculated (EXP1) aerosol peak surface area density (square micrometers per cubic centimeter) and peak aerosol mass (parts per billion by mass) as a function of time after the El Chichón eruption near 40°N. Measured aerosol surface area is from *Hofmann and Solomon* [1989], and measured aerosol mass is from *Hofmann and Rosen* [1984].

and mass reach a maximum 8–9 months after the eruption, which is about 1–2 months earlier than suggested by the measurements. A possible explanation is that the meridional transport is more vigorous in the model than in the atmosphere. In EXP2 the calculated maximum area, approximately 25 μm^2 cm^{-3}, is close to the observations. However, the calculated maximum mass density is about 30 ppbm, i.e., a factor of 2 lower than the observation. Calculated maximum area and mass densities are 35–60 times larger than the calculated background values and are quantitatively similar to the observations. We note that a secondary maximum is visible in the observed aerosol area (Figure 9a) but is not apparent in the observed aerosol mass (Figure 9b). The nature of these inconsistencies is not clear.

Figure 10 shows that in the EXP1 case, the calculated aerosol mass and area densities are significantly lower than the observations. In summary, the assumption that the total sulfur S emitted by the eruption of El Chichón is purely in the form of gas phase SO_2 results in a calculated volcanic aerosol load that is significantly lower than that suggested by the observations. However, with the assumption that 20% of the sulfur is released as sulfate particles, the model simulation is significantly improved. Thus in the following sections we will concentrate our discussion on the model results obtained from the EXP2 case.

4.5. Size Distribution of Volcanic Aerosols

Figure 11 represents the simulated aerosol size distributions at the equator at an altitude of 20 km, where the center of the volcanic cloud is located. We see that immediately after the eruption, the aerosol density corresponding to the smaller size particles rapidly increases. (A maximum aerosol density of about 300 # cm^{-3} μm^{-1}, corresponding to a size of 0.06 μm, is predicted.) Six months after the eruption the total number of aerosol particles starts to decay as result of transport and sedimentation processes. Aerosol densities at

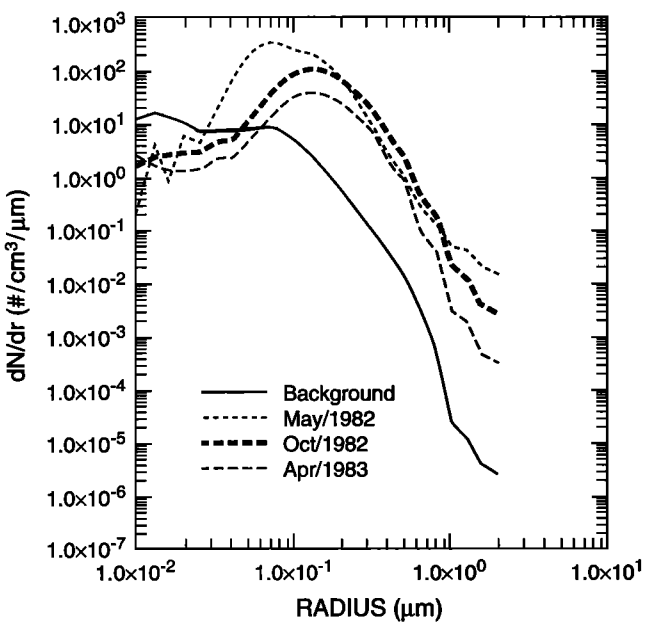

Figure 11. Simulated aerosol size distribution $dN(dr)/dr$ (# per cubic centimeter per micrometer) before and after the El Chichón eruption at the equator at 20 km.

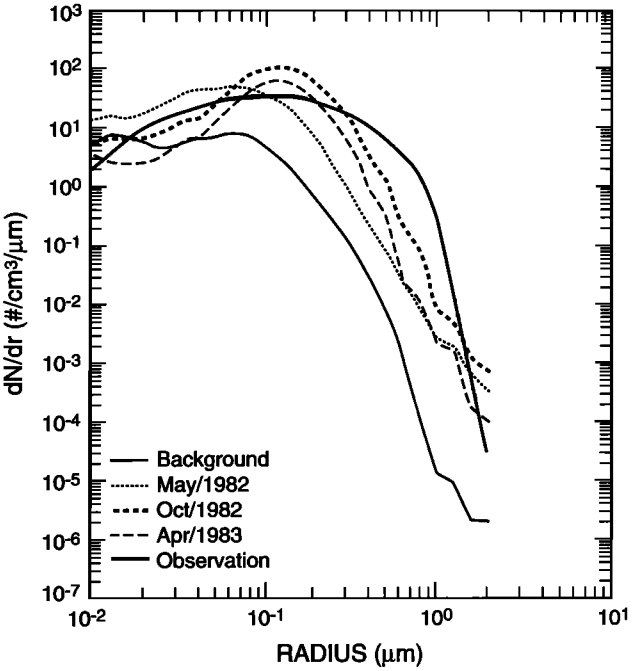

Figure 12. Calculated aerosol size distribution $dN(dr)/dr$ (# per cubic centimeter per micrometer) before and after the El Chichón eruption at 40°N and 20 km. Measured aerosol size distribution [*Hofmann and Solomon*, 1989] in January 1983 at 20 km and 41°N is also shown.

0.2–1 μm continue to grow through the coagulation process. A maximum aerosol density of about 100 # cm^{-3} μm^{-1} corresponds to a size of 0.2 μm. One year after the eruption the aerosol concentration decreases in the entire size spectrum, primarily as a result of gravitational sedimentation and transport processes; however, the concentrations corresponding to sizes greater than 0.1 μm are still above the background aerosol concentrations.

Figure 12 shows the simulated aerosol size distributions at 40°N at an altitude of 20 km. Significant differences in the aerosol size distribution at the equator are apparent. For example, at midlatitudes the aerosol concentration reaches its maximum a few months after the eruption, while at the equator it reaches its maximum 1 month after the eruption. In addition, a year after the eruption the aerosol concentration at the equator starts to decrease. At this time the aerosol size distribution at 40°N is similar to that at the equator, indicating that transport processes tend to make the aerosol distribution more uniform. The aerosol size distribution [*Hofmann and Solomon*, 1989] observed in January 1983 falls in the range of the aerosol size distributions calculated between October 1982 and April 1983, except for the sizes ranging from 0.7 μm to 1.0 μm, for which observed aerosol concentrations are higher than the calculated ones.

4.6. Simulated SO_2 Cloud

The calculated evolution of the SO_2 cloud helps us understand the conversion of SO_2 to sulfate aerosol. After the volcanic injection of a large amount of gas phase SO_2 into the atmosphere, an SO_2 cloud is produced in the tropics. Figure 13 shows that 1 month after the eruption, SO_2 has increased from a background concentration of 10 ppt (at 25 km, 10°N) to about 20 ppb. SO_2 is then converted to sulfate

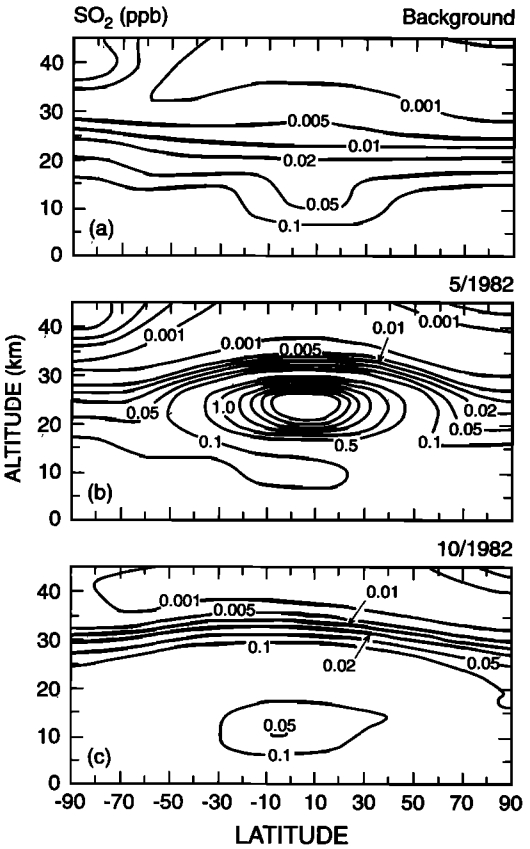

Figure 13. Simulated SO_2 concentration (parts per billion by volume) calculated as a function of latitude and altitude before (background) and after (May 1982 and October 1982) the eruption of El Chichón.

aerosol by chemical and microphysical processes so that its concentration decreases progressively. Figure 13c shows that the SO_2 concentration returns to its background level 6 months after the eruption. This conversion process after the eruption appears to be confirmed by observations. *Winker and Osborn* [1992] have shown that 1 month after the eruption of Mount Pinatubo, about half the SO_2 had been converted into sulfate aerosols. *Goldman et al.* [1992] observed that SO_2 concentrations were reduced by about 80% 3 months after the same eruption. Three to eight months after the eruption of El Chichón, *Vedder et al.* [1983] measured a concentration of SO_2 ranging from 0.03 ppb to 0.1 ppb at 20 km at midlatitude. Thus the measurements are consistent with the calculated evolution of the SO_2 cloud (EXP2) and suggest that SO_2 was rapidly converted to sulfate aerosols after the eruption as in EXP2.

4.7. Simulated Global Distribution of Aerosol Mass and Surface Area

In recent years, concern has been expressed about the impact of volcanic aerosols on stratospheric ozone [*Hofmann and Solomon*, 1989; *Prather*, 1992; *Brasseur and Granier*, 1992; *Kinne et al.*, 1992]. One of the possible impacts is that volcanic aerosols could produce local heating in the tropics of the lower stratosphere mainly as a result of infrared radiation absorption [*Kinne et al.*, 1992]. In this case the stronger upward motion resulting from tropical heating could lead to a reduction in the ozone column abundance [*Brasseur and Granier*, 1992]. Another possible impact is that the surface area available for heterogeneous reactions in the atmosphere is enhanced, so that it increases the conversion of inactive chlorine to active chlorine, which leads to enhanced ozone destruction [*Hofmann and Solomon*, 1989; *Prather*, 1992; *Brasseur and Granier*, 1992]. To assess these effects, a distribution of volcanic aerosols evolving with time is needed.

In Figure 14 we show the global distributions of the aerosol area density, which is a key parameter in evaluating the rates of heterogeneous chemical reactions. One month after the eruption of El Chichón the surface area reaches a maximum of about 50 μm^2 cm^{-3} at the equator near 23 km, which is consistent with the observation of 50 μm^2 cm^{-3} made in south Texas a few months after the eruption of El

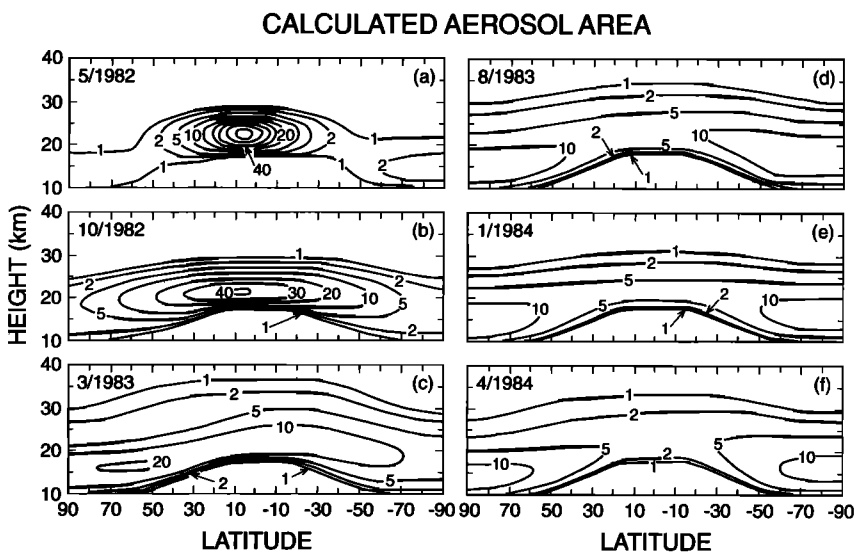

Figure 14. Calculated distribution of the total aerosol surface area density (square micrometer per cubic centimeter) after the eruption of El Chichón.

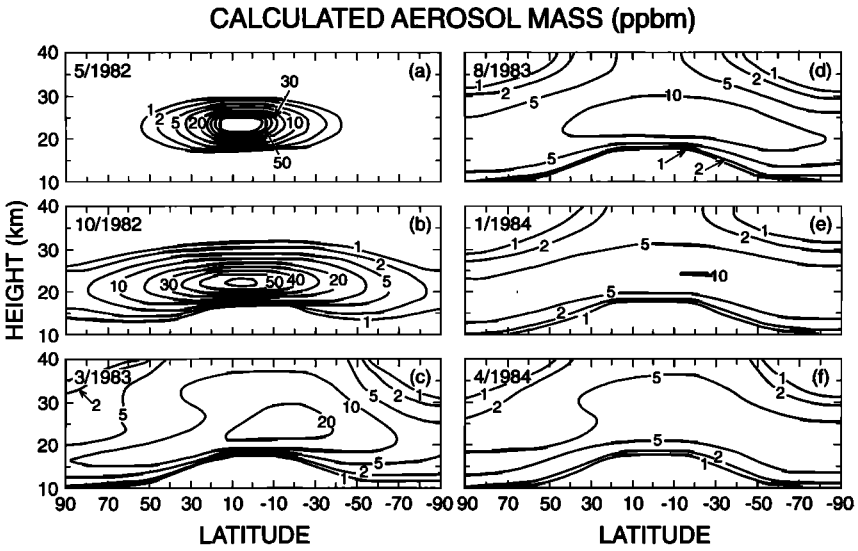

Figure 15. Calculated distribution of total aerosol mass density (parts per billion by mass) after the eruption of El Chichón.

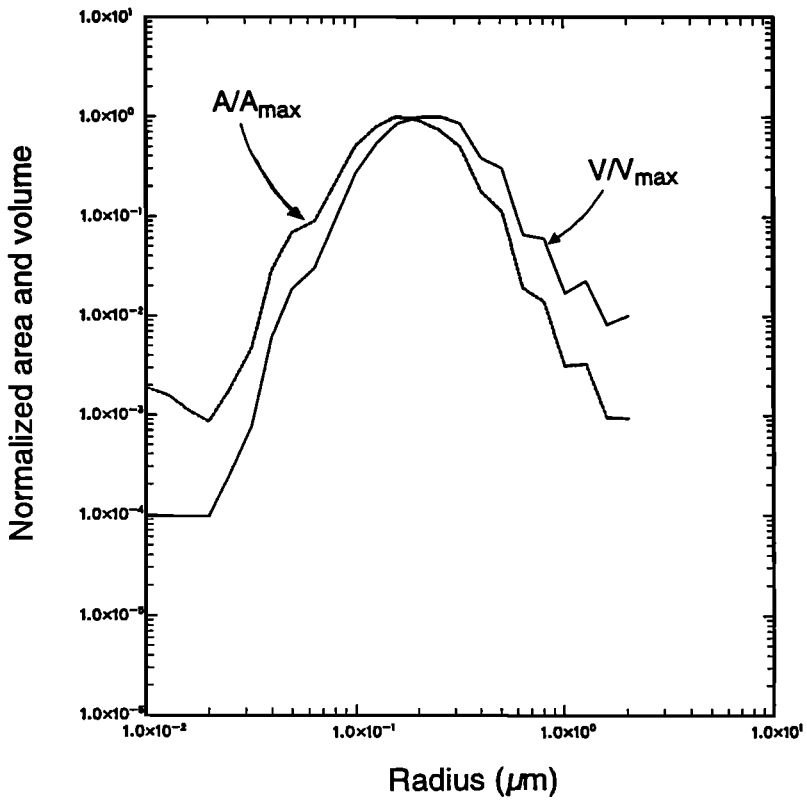

Figure 16. Calculated aerosol surface area and volume densities as a function of radius r at 15 km near the north pole in September 1983.

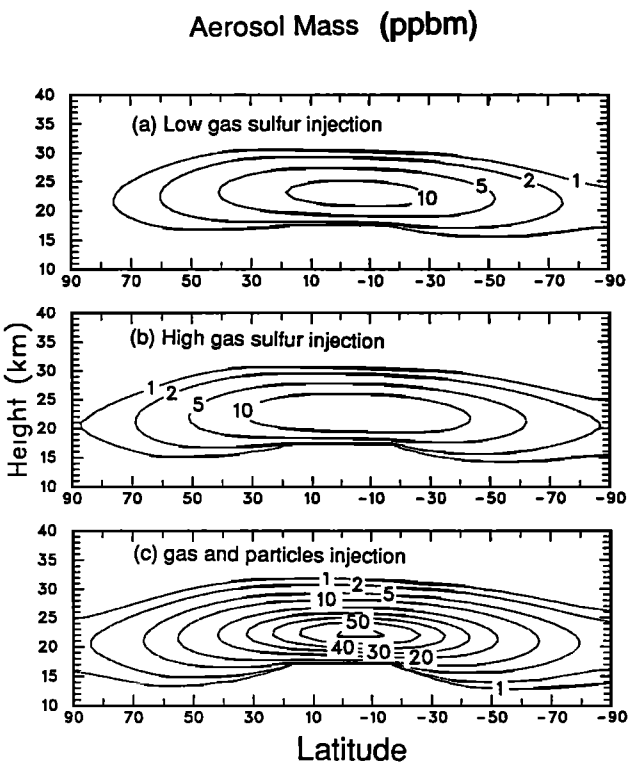

Figure 17. Simulated global distribution of aerosol mass density (parts per billion by mass) for (a) low injection of gas phase sulfur (EXP1), (b) high injection of gas phase sulfur (EXP3), and (c) low injection of gas phase and sulfate particles (EXP2) in September 1982. Low injection corresponds to 7 Tg sulfate, and high injection to 11 Tg sulfate.

Chichón [see *Hofmann and Solomon*, 1989]. Six months after the eruption the calculated aerosol area increases at mid to high latitudes and reaches approximately 20 μm^2 cm^{-3} at 40°N and 20 km and 5 μm^2 cm^{-3} at both the south and the north poles at altitudes of 10–23 km. Thirteen months after the eruption the peak in the aerosol surface area found earlier in the tropical lower stratosphere has disappeared, and the aerosol area (above 10 μm^2 cm^{-3}) is relatively uniform in the altitude range of 10 to 20 km. Sixteen months after the eruption a maximum of approximately 10 μm^2 cm^{-3} (10–20 times the background value) appears at high latitudes in both hemispheres. Twenty-two months after the eruption the area starts to decrease globally. Two years after the eruption the maximum remains at about 10 μm^2 cm^{-3} in the polar regions. The model therefore suggests that the heterogeneous reactions which are most efficient at high latitudes [*Granier and Brasseur*, 1992], where the photolysis of HNO_3 is slow and temperatures are low, could have played a significant role in ozone chemistry within about 6 months to 2 years after the El Chichón eruption. Perturbations in the ozone layer over a similar period seem to have occurred after the eruption of Mount Pinatubo [*Gleason et al.*, 1993].

Finally, Figure 15 shows the calculated global aerosol mass distribution. Between 1 and 6 months after the eruption the aerosol mass is highest near the equator at altitudes ranging from 20 to 25 km (about 50–100 times the value for background aerosols). The aerosol mass then decreases rapidly during the year following the eruption. Because the volcanic aerosol effects on ozone due to the radiative heating perturbation are confined to the tropics [*Labitzke and McCormick*, 1992; *Brasseur and Granier*, 1992; *Schoeberl et al.*, 1993], the effects of the El Chichón on ozone through the radiative heating should be important only during the first year following the eruption.

Comparing Figure 14 with Figure 15, we note that the temporal distributions of the aerosol mass and surface area density are characterized by different features in the polar regions, approximately $1\frac{1}{2}$ years after the eruption. The aerosol surface area density is largest at both poles, while the aerosol mass density is rather uniformly distributed through all latitudes. The reason is that $1\frac{1}{2}$ years after the eruption the largest aerosol particles are removed from the stratosphere by sedimentation and that the smaller aerosol particles become dominant in the polar regions. Figure 16 presents the aerosol surface area and volume calculated as a function of aerosol radius at 15 km near the north pole in September 1983. It shows that the surface area density (r^2 dependence) is dominated by particles smaller than those that determine the mass density (r^3 dependence). The maximum in surface area density is provided by particles with radius of 0.15 μm, and the maximum in volume (or mass density) resulted from particles with radius of 0.25 μm. It is the domination of the smaller aerosol particles on surface area which produces the maximum value calculated in the polar region $1\frac{1}{2}$ years after the eruption.

4.8. Sensitivity to Sulfur Injection

As we mentioned in section 4.1, there is a large uncertainty in the amount of sulfur injected into the stratosphere by the eruption. In EXP2 we shifted the partitioning between gas phase sulfur and sulfate particles injected but did not change the total amount of the injection. In order to account for the uncertainty in the total sulfur injection, we conduct a third calculation (EXP3) in which the total amount is 7.2 Tg (or 11 Tg in sulfate; see Table 2). The total injection is assumed to include only gas phase sulfur. Figure 17 shows the calculated aerosol mass in the three cases, i.e., low injection of gas phase sulfur (EXP1), low injection of sulfur including direct injection of aerosol particles (EXP2), and high injection of gas phase sulfur (EXP3) in September 1982. As discussed in section 4.2, the injection of gas phase sulfur prescribed in EXP1 underestimates the aerosol loading following the eruption. With a higher injection of gas phase sulfur (EXP3) the improvement in the calculation is not significant. It is only when a direct injection of aerosol particles (EXP2) is included in the model that the aerosol load is in good agreement with available observations. This sensitivity study provides additional support for the importance of direct injection of aerosol particles relative to eruptions.

5. Summary and Conclusion

The NCAR coupled dynamical/chemical/microphysical two-dimensional model reproduces reasonably well the distribution and fate of background and volcanic aerosols observed in the stratosphere. Because volcanic aerosols play an important role in the global climate and affect the chemistry of ozone in the stratosphere, it is important that

assessment models simulate accurately the evolution of the sulfate aerosol layer following large volcanic eruptions.

Immediately after the volcanic eruption of El Chichón, large quantities of sulfate aerosol were produced in the lower stratosphere. As suggested by the model calculations, approximately 20% of the sulfate aerosols could have been provided by direct injection of aerosols during the eruption, while the remaining 80% have been produced by the conversion of gas phase SO_2.

Acknowledgments. The authors thank Anne Smith, Alan Fried, Ian Folkins, Bruce Briegleb, and two anonymous reviewers for valuable comments. Thanks go to Janet Rodina for editorial assistance. This research was funded in part by the National Aeronautics and Space Administration under the program "The Atmospheric Effects of Stratospheric Aircraft: Modeling and Measurement in Support of the High-Speed Research." G.B. is supported in part at the University of Brussels by the Global Change Program of the Belgian government. X. Lin is supported in part by the Atmospheric Chemistry Project of the Climate and Global Change Program of the National Oceanic and Atmospheric Administration. The National Center for Atmospheric Research is sponsored by the National Science Foundation.

References

Ayers, G. P., R. W. Gillett, and J. L. Gras, On the vapor pressure of sulfuric acid, *Geophys. Res. Lett.*, *7*, 433–436, 1980.

Bekki, S., and J. A. Pyle, Two-dimensional assessment of the impact of aircraft sulphur emissions on the stratospheric sulphate aerosol layer, *J. Geophys. Res.*, *97*, 15,839–15,847, 1992.

Bojkov, R. D., The 1983 and 1985 anomalies in the ozone distribution in perspective, *Mon. Weather Rev.*, *115*, 2187–2201, 1987.

Brasseur, G., and C. Granier, Mount Pinatubo aerosols, chlorofluorocarbons, and ozone depletion, *Science Paris*, *257*, 1239–1242, 1992.

Brasseur, G., M. H. Hitchman, S. Walters, M. Dymek, E. Falise, and M. Pirre, An interactive chemical dynamical radiative two-dimensional model of the middle atmosphere, *J. Geophys. Res.*, *95*, 5639–5655, 1990.

Cadle, R. D., A. L. Lazrus, and J. P. Shedlovsky, Comparison of particles in the plume from eruptions of Kilauea, Mayon, and Arenal volcanoes, *J. Geophys. Res.*, *74*, 3372–3378, 1969.

Cadle, R. D., C. S. Kiang, and J.-F. Louis, The global scale dispersion of the eruption clouds from major volcanic eruptions, *J. Geophys. Res.*, *81*, 3125–3132, 1976.

Cadle, R. D., A. L. Lazrus, B. J. Huebert, L. E. Heidt, W. I. Rose, Jr., D. C. Woods, R. L. Chuan, R. E. Stoiber, D. B. Smith, and R. A. Zielinski, Atmospheric implications of studies of Central American volcanic eruption clouds, *J. Geophys. Res.*, *84*, 6961–6968, 1979.

Capone, L. A., O. B. Toon, R. C. Whitten, R. P. Turco, C. A. Riegel, and K. Santhanam, A two-dimensional model simulation of the El Chichón volcanic eruption cloud, *Geophys. Res. Lett.*, *10*, 1053–1056, 1983.

Crutzen, P. J., The possible importance of OCS for the sulfate layer of the stratosphere, *Geophys. Res. Lett.*, *3*, 73–76, 1976.

Deshler, T., A. Adriani, G. P. Gobbi, D. J. Hofmann, G. D. Donfrancesco, and B. J. Johnson, Volcanic aerosol and ozone depletion within the Antarctic polar vortex during the austral spring of 1991, *Geophys. Res. Lett.*, *19*, 1819–1822, 1992.

Devine, J. D., H. Sigurdaaon, A. N. Davis, and S. Self, Estimate of sulfur and chlorine yield to the atmosphere from volcanic eruptions and potential climate effects, *J. Geophys. Res.*, *89*, 6309–6325, 1984.

Fuchs, N. A., *The Mechanics of Aerosols*, Macmillan, New York, 1964.

Gleason, J. F., et al., Record low global ozone in 1992, *Science*, *260*, 523–526, 1993.

Goldman, A., F. J. Murcray, C. P. Rinsland, R. D. Blatherwick, S. J. David, F. H. Murcray, and D. G. Murcray, Mt. Pinatubo SO_2 column measurements from Mauna Loa, *Geophys. Res. Lett.*, *19*, 183–186, 1992.

Granier, C., and G. Brasseur, Impact of heterogeneous chemistry on model predictions of ozone changes, *J. Geophys. Res.*, *97*, 18,015–18,033, 1992.

Hamill, P., The time dependent growth of H_2O-H_2SO_4 aerosols by heteromolecular condensation, *J. Aerosol Sci.*, *6*, 475–482, 1975.

Hamill, P., O. B. Toon, and C. S. Kiang, Microphysical processes affecting stratospheric aerosol particles, *J. Atmos. Sci.*, *34*, 1104–1119, 1977.

Hirono, M., and T. Shibata, Enormous increase of stratospheric aerosols over Fukuoka due to volcanic eruption of El Chichón in 1982, *Geophys. Res. Lett.*, *10*, 152–154, 1983.

Hobbs, P. V., L. F. Radke, and J. L. Stith, Particles in the eruption cloud from St. Augustine volcano, *Science*, *199*, 457–458, 1978.

Hofmann, D. J., and S. J. Oltmans, The effect of stratospheric water vapor on the heterogeneous reaction rate of $ClONO_2$ and H_2O for sulfuric acid aerosol, *Geophys. Res. Lett.*, *19*, 2211–2214, 1992.

Hofmann, D. J., and J. M. Rosen, On the temporal variation of stratospheric aerosol size and mass during the first 18 months following the 1982 eruptions of El Chichón, *J. Geophys. Res.*, *89*, 4883–4890, 1984.

Hofmann, D. J., and S. Solomon, Ozone destruction through heterogeneous chemistry following the eruption of El Chichón, *J. Geophys. Res.*, *94*, 5029–5041, 1989.

Hoppel, W. A., Growth of condensation nuclei by heteromolecular condensation, *J. Rech. Atmos.*, *9*, 167–180, 1976.

Jet Propulsion Laboratory (JPL), Chemical kinetics and photochemical data for use in stratospheric modeling, *JPL Publ. 90-1*, Pasadena, Calif., 1990.

Kasten, F., Falling speed of aerosol particles, *J. Appl. Meteorol.*, *7*, 944–947, 1968.

Kinne, S., O. B. Toon, and M. J. Prather, Buffering of stratospheric circulation by changing amounts of tropical ozone: A Pinatubo case study, *Geophys. Res. Lett.*, *19*, 1927–1930, 1992.

Labitzke, K., and M. P. McCormick, Stratospheric temperature increases due to Pinatubo aerosols, *Geophys. Res. Lett.*, *19*, 207–210, 1992.

McCormick, M. P., and T. J. Swissler, Stratospheric aerosol mass and latitudinal distribution of the El Chichón eruption for October 1982, *Geophys. Res. Lett.*, *10*, 877–880, 1983.

McCormick, M. P., T. J. Swissler, W. H. Fuller, W. H. Hunt, and M. T. Osborn, Airborne and ground-based lidar measurements of the El Chichón stratospheric aerosol from 90°N to 56°S, *Geofis. Int.*, *23*(2), 187–221, 1984.

McKeen, S. A., S. C. Liu, and C. S. Kiang, On the chemistry of stratospheric SO_2 from volcanic eruptions, *J. Geophys. Res.*, *89*, 4873–4881, 1984.

Mroz, E. J., A. S. Mason, and W. A. Sedlacek, Stratospheric sulfate from El Chichón and the mystery volcano, *Geophys. Res. Lett.*, *10*, 873–876, 1983.

Mroz, E. J., A. S. Mason, R. Leifer, and Z. R. Juzdan, Stratospheric impact of El Chichón, *Geofis. Int.*, *23*(3), 321–333, 1984.

Murrow, P. J., W. I. Rose, Jr., and S. Self, Determination of the total grain size distribution in a vulcanian eruption column and its implication to stratospheric aerosol perturbation, *Geophys. Res. Lett.*, *7*, 893–896, 1980.

Newell, R. E., and H. B. Selkirk, Recent large fluctuations in total ozone, *Q. J. R. Meteorol. Soc.*, *114*, 595–617, 1988.

Pinto, J. P., R. P. Turco, and O. B. Toon, Self-limiting physical and chemical effects in volcanic eruption clouds, *J. Geophys. Res.*, *94*, 11,165–11,174, 1989.

Prather, M., Catastrophic loss of stratospheric ozone in dense volcanic clouds, *J. Geophys. Res.*, *97*, 10,187–10,191, 1992.

Rose, W. I., R. L. Chuan, and D. C. Woods, Small particles in plumes of Mount St. Helens, *J. Geophys. Res.*, *87*, 4956–4962, 1982.

Rosen, J. M., D. J. Hofmann, and J. Laby, Stratospheric aerosol measurements, II, The world-wide distribution, *J. Atmos. Sci.*, *32*, 1457–1462, 1975.

Schoeberl, M. R., P. K. Bhartia, E. Hilsenrath, and O. Torres, Tropical ozone loss following the eruption of Mt. Pinatubo, *Geophys. Res. Lett.*, *20*, 29–32, 1993.

Sedlacek, W. A., E. J. Mroz, A. L. Lazrus, and B. W. Gandrud, A decade of stratospheric sulfate measurements compared with observations of volcanic eruptions, *J. Geophys. Res.*, *88*, 3741–3776, 1983.

Steele, H. M., and P. Hamill, Effects of temperature and humidity

on the growth and optical properties of sulfuric acid–water droplets in the stratosphere, *J. Aerosol Sci.*, *12*, 517–528, 1981.

Turco, R. P., P. Hamill, O. B. Toon, R. C. Whitten, and C. S. Kiang, A one-dimensional model describing aerosol formation and evolution in the stratosphere, I, Physical processes and numerical analogs, *J. Atmos. Sci.*, *36*, 699–717, 1979.

Turco, R. P., R. C. Whitten, and O. B. Toon, Stratospheric aerosols: Observation and theory, *Rev. Geophys.*, *20*, 233–279, 1982.

Turco, R. P., O. B. Toon, R. C. Whitten, P. Hamill, and R. G. Keesee, The 1980 eruptions of Mount St. Helens: Physical and chemical processes in the stratospheric clouds, *J. Geophys. Res.*, *88*, 5299–5319, 1983.

Twomey, S., *Atmospheric Aerosols*, Elsevier Science, New York, 1977.

Vedder, J. F., E. P. Condon, E. C. Y. Inn, K. D. Tabor, and M. A. Kritz, Measurements of stratospheric SO_2 after the El Chichón eruptions, *Geophys. Res. Lett.*, *10*, 1045–1048, 1983.

Visconti, G., M. Verdecchia, and G. Pitari, A comparison of lidar data and two-dimensional simulation of dust transport from the eruption of El Chichón, *J. Atmos. Sci.*, *45*, 1097–1109, 1988.

Winker, D. M., and M. T. Osborn, Airborne lidar observations of the Pinatubo volcanic plume, *Geophys. Res. Lett.*, *19*, 167–170, 1992.

Woods, D. C., and R. L. Chuan, Fine particles in the Soufrière eruption plume, *Science*, *216*, 1118–1119, 1982.

World Meteorological Organization (WMO), *Scientific Assessment of Ozone Depletion: 1991*, Geneva, 1992.

Yue, G. K., and P. Hamill, The homogeneous nucleation rates of H_2SO_4-H_2O aerosol particles in air, *J. Aerosol Sci.*, *10*, 609–614, 1979.

G. Brasseur and X. Tie, National Center for Atmospheric Research, P. O. Box 3000, Boulder, CO 80303.

X. Lin, Aeronomy Laboratory, Environmental Research Laboratory, NOAA, Boulder, CO 80303.

(Received August 26, 1993; revised March 11, 1994; accepted April 26, 1994.)